

**Solar Spicules:
A Review of Recent Models
and Targets for Future Observations**

Alphonse C. Sterling¹

NASA/Marshall Space Flight Center, SD50/Space Science
Department, Huntsville, AL 35812
asterling@solar.stanford.edu

Solar Physics, 196, 79 (2000)

¹ NRC—MSFC Research Associate

Abstract

Since their discovery over 100 years ago, there have been many suggestions for the origin and development of solar spicules. Because the velocities of spicules are comparable to the sound and Alfvén speeds of the low chromosphere, linear theory cannot fully describe them. Consequently, detailed tests of theoretical ideas had to await the development of computing power that only became available during the 1970s. This work reviews theories for spicules and spicule-like features over approximately the past 25 years, with an emphasis on the models based on nonlinear numerical simulations. These models have given us physical insight into wave propagation in the solar atmosphere, and have helped elucidate how such waves, and associated shock waves, may be capable of creating motions and structures on magnetic flux tubes in the lower solar atmosphere. So far, however, it has been difficult to reproduce the most-commonly-quoted parameters for spicules with these models, using what appears to be the most suitable input parameters. A key impediment to developing satisfactory models has been the lack of reliable observational information, which is a consequence of the small angular size and transient lifetime of spicules. I close with a list of key observational questions to be addressed with space-based satellites, such as the currently operating *TRACE* satellite, and especially the upcoming Solar-B mission. Answers to these questions will help determine which, if any, of the current models correctly explains spicules.

1 Introduction

Spicules comprise one of the most fundamental components of the solar chromosphere. They appear to be jets of gas seen at the limb of the Sun in chromospheric spectral lines, and have been observed in $H\alpha$ and other chromospheric spectral lines for over 100 years. They have an upward mass flux 100 times that of the solar wind, and therefore are an important consideration in the mass balance of the solar atmosphere. Their disk representation is uncertain, but fibrils and the bright and dark mottles must be at least related to spicules. Paraphrasing Osterbrock (1961) and Foukal (1990): spicules are a fascinating challenge from the theoretical and numerical approach, as they apparently require us to explain how chromospheric material can be raised to heights greater than those expected from ballistic motions, without raising the material to temperatures greater than those characteristic of the chromosphere, about 10^4 K.

There have been many attempts to theoretically explain how spicules are created. Here I review more recent models, especially those developed over the past couple of decades. Beckers (1968, 1972), Bray et al. (1974), Athay (1976), and Campos (1984) summarize earlier models, and Sterling (1998a) briefly reviews numerical models. Most of the early models were, necessarily, largely descriptive or analytical in nature. Because the (apparent) velocities of spicules are similar to the sound and Alfvén velocities of the photospheric and chromospheric regions where they exist, however, nonlinear methods are required to describe in detail the response of the solar atmosphere to the suggested driving processes. As a result, non-linear numerical simulations have opened up a whole new, and productive, avenue for investigating hydrodynamic and magnetohydrodynamic (MHD) problems related to spicules.

With the growing development and use of computers since the late 1970s, there have been several attempts to describe the origin and evolution of spicules using non-linear numerical simulations. In this review I will emphasize these numerical models, and only briefly mention some of the other analytical studies and less-well-developed proposals. This emphasis is

primarily due to my background experience, and does not mean I believe that non-numerical approaches are less viable. Indeed, there are limitations to numerical models also, including, for example, complexities such as magnetic field properties, the form of the energy equation, etc. Moreover, some analytical approaches address the question of the ultimate energy source of spicules (see §4), which is often only included as an assumed parameter in numerical models.

All of the simulations begin with some form of deposition of energy in the photospheric or chromospheric portion of a magnetic flux tube which extends from the photosphere into the corona. As a consequence of the energy deposition, chromospheric matter is driven into the corona, and in many cases that uplifted material has properties roughly matching those observed in spicules. Just how well the simulations match the observations depends upon the form and location of the energy deposition. Three types of energy deposition processes have been examined in detail: (a) A velocity or pressure pulse applied to the photospheric or chromospheric material near the base of the flux tube. A velocity pulse could be a natural consequence of a convective flow manifested in granular motions interacting with material at the base of the flux tube, while a pressure pulse may result from an energy release due to, e.g., reconnection between small-scale magnetic elements. (b) A pressure pulse released in a localized region in the flux tube in the middle or upper chromosphere, again perhaps due to reconnection, or to some other energy source that may drive the brightenings seen in the chromosphere and transition region. (c) Alfvén waves generated by twists or disturbances at the base of the magnetic flux tubes; as with case (a), these perturbations may be a result of granules striking the magnetic flux tube.

I will not attempt a detailed discussion of spicule observations, although I will briefly summarize observed spicule properties in §2, and cite some of the more recent observational findings where appropriate. In §3 I review models of spicules based upon numerical simulations; in §4 I briefly discuss analytical investigations and some additional ideas; §5 contains discussions of features similar to spicules; in §6 I present thoughts on our state of theoretical understanding of spicules, and in §7 I conclude with a list of some of the most fundamental outstanding questions to be resolved observationally.

2 Overview of Spicule Properties

Spicules have widths near the limit of resolution for instruments thus far used to study them. Consequently, many of their properties are uncertain, with observational results frequently conflicting. Of course, such uncertainties and conflicts compound the theoretical modeling problem. Beckers (1968, 1972), Bray et al. (1974), Michard (1974), Athay (1976), and dePontieu (1996) provide comprehensive reviews of properties of spicule and spicule-like structures. Some recent observational studies are Cuny (1987); Braun et al. (1987); Matsuno et al. (1988); Nishikawa (1988); and Heristchi et al. (1992). Recent studies of spicule-like disk features include Heinzl et al. (1994), Tsiropoula (1994), Suematsu et al. (1995); Tsiropoula et al. (1997), Suematsu (1998), and Zachariadis et al. (1999). These disk features, also called mottles or fibrils, may or may not be spicules, but they must be at least related (see §5.) Although these disk features are also occasionally referred to as spicules (e.g., Zirin 1988; Suematsu et al. 1995, Suematsu 1998), I will retain the more common usage for spicule: the common jet-like features seen at the limb in chromospheric spectral lines.

Beckers (1968, 1972) gives the reported average projected heights for spicules to be between 6500 and 9500 km. But the distribution of heights is broad. For example, Lippin-

cott (1957) gives heights of 7,000—13,000 km for the majority of spicules, and according to Bray et al. 1974) these values are probably the best available. Most spicules have widths of $\lesssim 300$ —1500 km (Nishikawa 1988; Lynch et al. 1973; Ajmanova et al. 1982), lifetimes of ≈ 1 —10 minutes (Lippincott 1957; Bray et al. 1974), upward velocities of about 25 km s^{-1} , temperatures of about 5000—15,000 K, and densities of about $3 \times 10^{-13} \text{ g cm}^{-3}$. Their density and temperature variation with height is relatively constant; that is, their observed density and temperature scale heights are larger than those for a gas of comparable temperature in hydrostatic equilibrium. Some reports say that a substantial percentage of spicules do not retract after attaining maximum height. Rather, some of them “fade from view” in chromospheric spectral lines (e.g., Beckers 1968, 1972; but Suematsu et al. 1995, report that some 80% of the H α spicule-like disk features of their study are seen falling after rising). In any case, most of the material in the spicules must return to the surface, since the outward mass flux is much larger than that of the solar wind. Mottles on the disk cluster around supergranule cell boundaries, where the average magnetic field strength is enhanced.

There is uncertainty whether the upward velocity profiles of spicules are ballistic or constant. Rush et al. (1954) and Lippincott (1957) report that velocities are roughly constant, although variations and irregularities also were observed (cf. discussion in Bray et al. 1974); some of the irregularities may be due to seeing conditions. Hasan et al. 1984 also report no significant variation of spicule velocity with height. Athay et al. (1957) and Nishikawa (1988) point out that it is difficult or impossible to differentiate between constant and ballistic motions of limb spicules based on available data. Suematsu et al. (1995) note that a pure ballistic motion is unrealistic for the disk features they studied; this is because they do not observe the high initial velocities required for ballistic motion needed to reach typical spicule heights, and also the rise times for the features they observe are too long for pure ballistic motions. It is also possible, however, that development of the features at the lowest altitudes is not being observed, perhaps due to the small diameters of the magnetic flux tubes at those heights.

Regarding requirements for a spicule mechanism, as a minimum it must supply energy of the order of the amount needed to support spicules against gravity. For a fully extended spicule the potential energy is $mgh \lesssim 10^{25}$ erg, assuming a constant density of $\approx 3 \times 10^{-13} \text{ g cm}^{-3}$ along the spicule length and corresponding mass, m , a height $h \approx 10,000$ km and diameter of ≈ 500 km, with g the acceleration of gravity at the Sun’s surface. Granules have diameters of $\sim 10^3$ km and horizontal and vertical velocities of ≈ 1.4 and 1.8 km s^{-1} , respectively (e.g., Foukal 1990), implying a kinetic energy of $\gtrsim 10^{27}$ erg. Moreover, the lifetime of a granule is comparable to that of a spicule. Thus there is adequate energy contained in granular motions to drive spicules, and their ubiquity makes them a natural candidate for the ultimate energy source of spicules (e.g., Roberts 1979; Roudier et al. 1994). Whether photospheric energy is actually converted to spicule motion either directly or indirectly (e.g., via distortions of the magnetic field), however, is still one of many outstanding questions.

3 Numerical Models

For this review, I classify the numerical spicule models into the following categories:

- Strong pulse in the lower atmosphere.
- Weak pulse in the lower atmosphere (Rebound Shock Model).

- Pressure-pulse in the higher chromosphere.
- Alfvén wave models.

Here, “lower atmosphere” refers to the photosphere or low chromosphere, and “higher chromosphere” refers to the middle or upper chromosphere.

So far nearly all of these simulations have been on one-dimensional (or 1.5 dimensions in the case of most of the Alfvén wave-related studies) geometries. This is partially justified by the apparent one-dimensional behavior of spicules, but no one can be sure how serious a limitation this is. It is interesting to note that long, thin coronal structures are commonly seen in the high-resolution *TRACE* images, and this may hint that 1-D is a valid approximation for understanding the dynamics of many solar features. So far, the non-Alfvén wave model calculations have all assumed a rigid magnetic flux tube.

Several of the models have been revisited repeatedly over the years by different workers using different computer codes. Different versions of the models have varying amounts of physics in them, but all include some form of the following equations:

$$\frac{\partial}{\partial t}(\rho A) + \frac{\partial}{\partial z}(\rho v A) = 0, \quad (1)$$

$$\frac{\partial}{\partial t}(\rho v A) + \frac{\partial}{\partial z}(\rho v^2 A) = -\rho g A - A \frac{\partial p}{\partial z} + F \rho A h(z, t), \quad (2)$$

and

$$\frac{\partial E}{\partial t} + \frac{1}{A} \frac{\partial}{\partial z} \left[(E + P)v A - \kappa A \frac{\partial T}{\partial z} \right] = -\rho v g - L + S + E h(z, t), \quad (3)$$

where

$$E = \frac{1}{2} \rho v^2 + \frac{p}{\gamma - 1}. \quad (4)$$

Equations 1–3 are, respectively, equations for the conservation of mass, momentum, and energy. In these equations, t , z , ρ , A , v , g , κ , T , L , and S represent, respectively, time, distance along the flux tube from the base, density, cross sectional area of the flux tube supporting the spicule, velocity, gravitational acceleration at the solar surface, coefficient of thermal conduction, temperature, radiation losses, and background heating rate needed to maintain the initial atmosphere. The momentum and energy equations contain terms for a driving force of magnitude F and an input energy term of magnitude E , respectively, with $h(z, t)$ describing how the quantities vary in space and time. In many of the simulations $F = 0$, in which case a driving force develops from the energy input term alone. In some simulations, effects of ionization are added via modifications to the energy equation and the addition of ionization equations. Simulations involving Alfvén waves also utilize Maxwell’s equations and include appropriate terms in the momentum and energy equations. An equation of state is added to close the system of equations.

Among the differences between models is the assumed geometry of the magnetic field on which the spicule is generated, specifically the cross sectional area as a function of z , $A(z)$; based on observations of strong magnetic elements in the photosphere, it is expected that the cross section expands out by a factor of ten or more in going from the photosphere into

the corona. Some models include this expansion while others omit it. Another difference has to do with including or omitting the effects of radiation and heat conduction via values for κ , L , and S . As pointed out by Foukal (1990), radiative losses in the chromosphere can have a damping effect on spicule mechanisms which rely on deposition of energy in the strongly-radiative low chromosphere. Simulations omitting cross sectional area variation or radiation losses are still important, as the calculations with less physics are extremely useful for elucidating the processes occurring in the more complicated systems. Moreover, there is still uncertainty in the nature of the physical conditions that make up spicules; for example, the appropriate form for the radiative loss rate, L , in spicules is not known. Therefore, one must be cautious to not over-interpret results obtained using any given set of assumptions for L .

3.1 Strong Pulse in the Low Atmosphere

This is the most straight-forward mechanism to consider for generating spicules: A sudden, strong pulse at the base of a vertical magnetic flux tube drives chromospheric material into the corona. Suematsu et al. (1982) studied this possibility using numerical simulations. They assumed that the strong pulse was due to a sudden pressure enhancement in the photosphere or low chromosphere, the motivation for this being observations of bright points in the chromospheric network.

They began with a simple, rigid magnetic flux tube of constant cross section ($A = 1$), as shown in Figure 1a, and solved appropriate forms of Equations 1–3; effects of radiation and heat conduction were not included (L , κ , and $S = 0$). An initial pressure pulse ($F = 0$, $E \neq 0$) generates a disturbance which nonlinearly steepens into a gas-dynamic shock (Fig. 1b). This shock can be considered as an MHD slow-mode shock for a very low-beta plasma, that is, where the magnetic field is rigid enough to not be affected by the gas motions. This shock interacts with the transition region, thrusting it upward, and the material behind the uplifted transition region is identified as the model spicule (Fig. 1c). Figure 1c shows that additional shocks form after elevation of the spicule. These shocks (called “rebound shocks” by Hollweg 1982) do not participate in the rise of the spicule in this scenario discussed here, but will be a key feature in the model discussed in §3.2.

In agreement with observations, the resulting model spicule has relatively flat density and temperature profiles in height. Adiabatic expansion of the upward-propagating material results in cool spicules, although the temperatures may just reach the lower end of the reported range of observed spicule temperatures. This model predicts a smooth trajectory for the top of the spicule during its ascent. Since the motion of the material is ballistic, it predicts initial velocities $\approx 60 \text{ km s}^{-1}$. As noted in §2, such large velocities have not been observed. How the predicted spicules will be modified by a varying magnetic field geometry and radiation losses has not yet been investigated.

Shibata et al. (1982a) apply the model to different initial atmospheric conditions, specifically, those corresponding to active regions and those corresponding to coronal holes. These regions have transition region heights that are respectively lower and higher than that of quiet regions. They find that a lower initial transition region height results in shorter-height spicules. This is because, with the lowered transition region, the shocks generated in the low chromosphere have a shorter length of chromosphere to travel through than with a higher initial transition region. Consequently, the resulting shocks do not grow to be as strong as they would with a higher transition region, resulting in a smaller force being imparted upon the

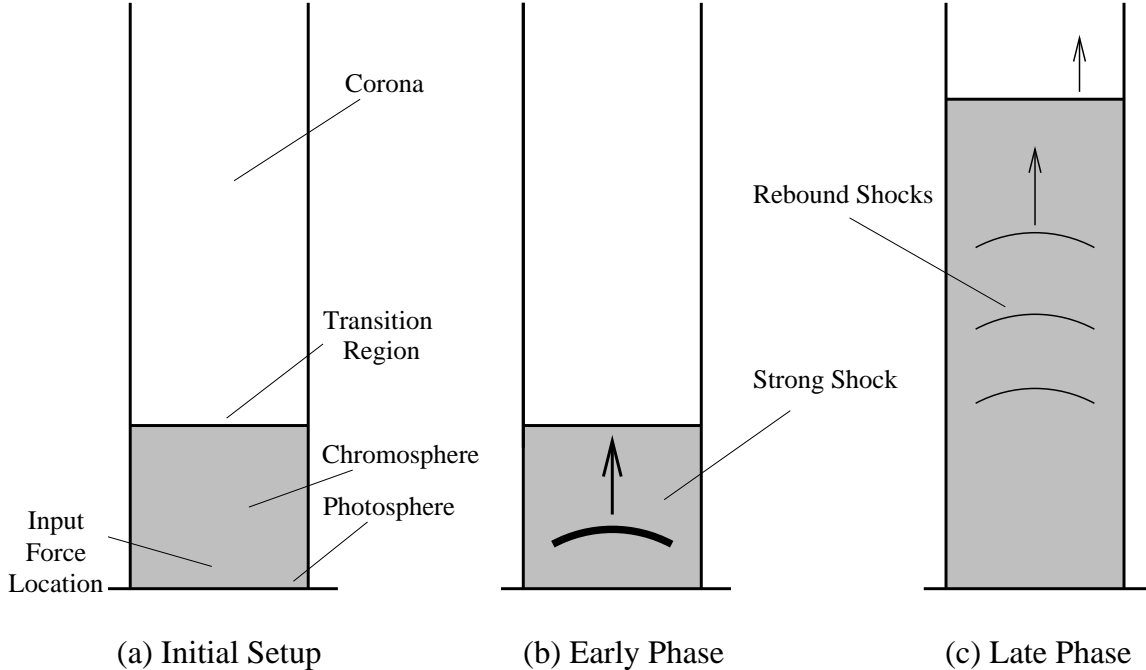


Figure 1: Schematic diagram of a model spicule produced by a pressure pulse in the low chromosphere. There is no area expansion of the flux tube with height in this case. Initially the transition region is at a height of about 2000 km. An initial pressure pulse near the photosphere creates a strong shock. This shock drives the transition region upward, creating a spicule-like feature in the late phases. Grey regions here and in other figures indicate cool, dense, chromospheric-type material. “Rebound shocks” form at later times, but they are not required to lift the spicule in this model.

transition region, and thus lower-height spicules. Similarly, spicules in coronal holes would be higher than those in quiet regions, due to a higher initial transition region height.

These findings are important in comparing with observations of spicules. Spicules are tall under polar regions (e.g., Beckers 1968, Rabin et al. 1980), where coronal holes are expected. Zirin (1988, p. 171) reports that spicules are absent over plages. These points are consistent with the Shibata et al. (1982a) results. Further clarification of the observational situation is wanting, however, as *TRACE* Fe IX/X 171 Å observations suggest that spicule-like chromospheric features may be present as “dark inclusions” in the EUV moss features, which occur in plage regions (Berger et al. 1999). In a comment in Michard (1974), Beckers remarks that it is not clear whether spicules are absent in plages.

3.2 Weak Pulse in the Low Atmosphere: Rebound Shock Model

Similar to the above idea, this model, first examined by Hollweg (1982), also begins with a pulse in the low chromosphere, but weaker in amplitude than that in the strong-pulse case. This weaker pulse could represent granules buffeting magnetic flux tubes, which would explain the ubiquitousness of spicules.

Hollweg (1982) examined this model assuming a rigid flux tube with expanding cross section extending from the photosphere into the corona, as sketched in Figure 2a. Rather

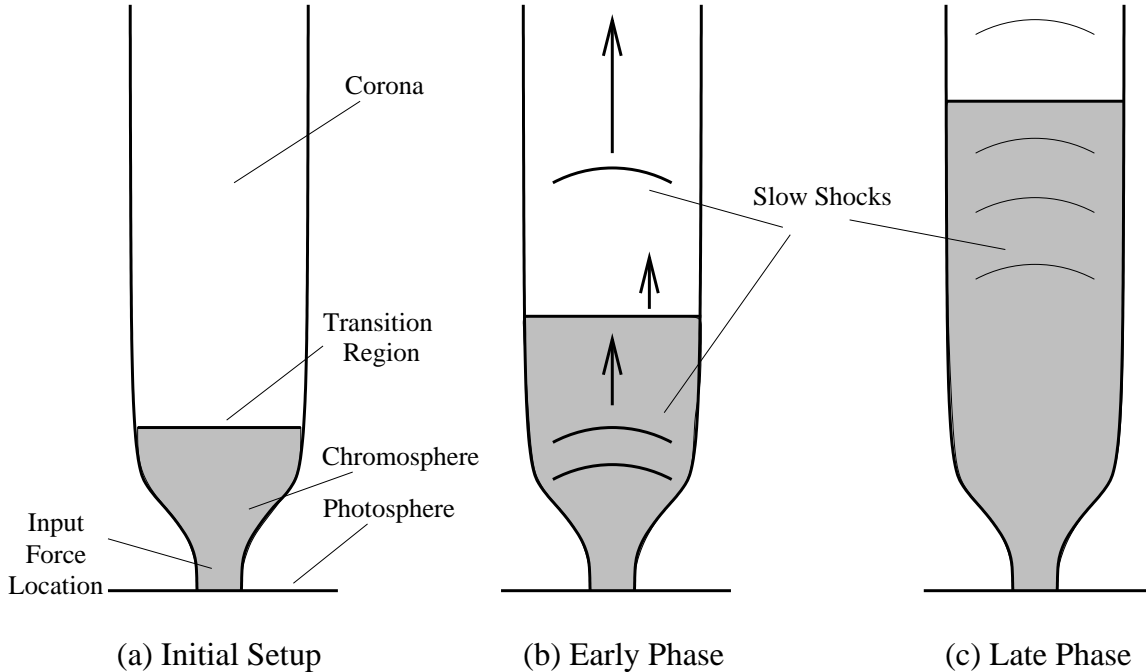


Figure 2: Schematic diagram of the Rebound Shock model for spicules. The initial atmosphere is similar to that of Fig. 1a, except the magnetic flux tube expands with height in this representation. A force is applied near the base of the flux tube. This leads to an initial slow shock, followed by a train of rebound shocks which continue to push the transition region upward. In 2c, this elevated material represents a mature spicule. In the last phases, the slow (rebound) shocks continue, but weaken with time.

than using a pressure pulse, he initiated the simulations using a velocity pulse of magnitude $\sim 1 \text{ km s}^{-1}$ (the magnitude seen in granular motions) applied to plasma in the photosphere or low-chromosphere at the base of the flux tube by a localized, transient force; thus he used $F \neq 0$ and $E \neq 0$ in Equations 2 and 3. Radiation losses and heat conduction were not included at this stage. Thus, the differences from the Suematsu et al. (1982) initial setup were the magnetic field cross-sectional variation, the form of the input force (velocity pulse instead of pressure pulse), and the magnitude of the input pulse.

In response to the velocity perturbation, the chromosphere launches an acoustic gravity wave train—consisting of a wave front followed by an oscillating wake—upward along the flux tube. That is, after the initial wave is launched, the chromosphere “rings” at its acoustic cutoff frequency (or “tube frequency”), as described in linear theory (e.g., Morse et al. 1953; Rae et al. 1982; Sterling et al. 1988); for the low solar atmosphere, this corresponds to periods of 200–300 s. Even though the initial velocity of the waves generated in the photosphere is low-amplitude, conservation of kinetic energy requires that the wave amplitudes grow because of the exponential dropoff of density with height in the chromosphere; non-linear effects become increasingly important as the wave amplitudes grow. Since the simulations are non-linear, the wave front and oscillating wake steepen into a stream of slow-mode MHD shocks propagating up the flux tube, as sketched in Figure 1b. These shocks are called “rebound shocks” since they form when a portion of the chromospheric gas uplifted by a previous shock falls due to

gravity, and then “rebounds” back upward again after compressing the chromospheric gas at lower heights. This rebound produces a new wave which steepens into a new shock, and the process is repeated. The initial and rebound shocks strike the transition region, propelling it and the chromospheric material below it into the corona (Fig. 1c). As in the previous model, the material beneath the uplifted transition region is identified with the spicule.

Physically, much of the evolution of the system is similar to the strong-pulse case, where, as noted above, rebound shocks also formed. The difference is that here the rebound shocks are an integral part of the rise of the spicule, whereas in the strong-pulse case the initial shock alone accounts for the rise of the spicule. Consequently, in this *rebound shock model*, the rise of the spicule is intermittent because the rebound shocks repeatedly accelerate the transition region upward. Hollweg (1982) suggests that this motion could appear as a non-ballistic, approximately constant-velocity rise of spicules if observed with insufficient resolution. Thus the initial velocities are substantially less than the $\approx 60 \text{ km s}^{-1}$ of the strong-pulse model which resulted in a ballistic rise for the spicule. Another difference is that the train of shocks results in substantially elevated model spicule temperatures, due to repeated shock heating overcoming the cooling due to adiabatic expansion. As noted in §2, non-ballistic motions and elevated spicule temperatures have been reported by some observers, but these points are still in question. (In addition to spicules, shock dissipation of acoustic waves is a suggested mechanism for the heating of the general chromosphere; see Narain et al. 1990, 1996,, and references therein.)

There have been a number of follow-up investigations of the rebound shock model for spicules. Sterling et al. (1988) extended the original Hollweg calculations in time and parameter space, and Sterling et al. (1990) added radiation losses and heat conduction to the vertical flux tube calculations. (The pressure gradient term in Equation 2 of Sterling et al. 1990 is incorrectly stated. It should read $A\partial p/\partial z$, rather than $\partial Ap/\partial z$. The calculations for that paper were carried out using the correct momentum equation, rather than the incorrectly-stated one.)

In a series of papers, Cheng further extended the model by (a) considering the consequences of the ionization of the spicule material (the material goes from nearly neutral to nearly fully ionized as heating occurs in the spicule) and variable molecular weight (which changes with the level of ionization in the spicule) in Cheng (1992a), by (b) utilizing a different form for the radiation losses in the chromosphere than that of Sterling et al. (1990) in Cheng (1992b), and by (c) examining the characteristics of the spicule plasmas as the material falls back to the chromosphere in Cheng (1992c). These calculations used velocity pulses of amplitude $\approx 1 \text{ km s}^{-1}$ in the Hollweg, Sterling and Hollweg, and Sterling and Mariska studies, and $\approx 1\text{--}3 \text{ km s}^{-1}$ for the Cheng studies. Hansteen et al. (1994) calculated expected properties of transition region emission lines for a version of the rebound shock model.

When radiation losses are included in the calculations, the situation regarding spicule formation becomes less optimistic. Sterling et al. (1990) were not able to generate tall (height $\gtrsim 6,000 \text{ km}$) features with velocities near those observed in spicules when radiation was included and realistic setup was used. They could reproduce such spicule properties only when they used the non-realistic assumption of a constant cross-section magnetic field. Cheng (1992a, 1992b) only considered a constant cross-section magnetic field, and generally used higher photospheric velocities than Sterling et al. (1990). His results confirm that radiation substantially alters the nature of the resulting spicule-like structures, but he also found that spicule properties are better reproduced when the input force is continued for a longer

time.

Thus, when radiation effects are ignored in the rebound shock model, spicule-like features can be produced with standard assumptions (photospheric velocities $\sim 1 \text{ km s}^{-1}$; magnetic flux-tube expansion with height). When standard models for atmospheric radiation losses are incorporated, however, spicule-like structures result only when (presumably) unrealistic assumptions regarding magnetic field geometry, and perhaps also photospheric velocities, are incorporated. Without such unrealistic assumptions, the calculations including radiation losses result in only small amplitude oscillatory motions of the transition region and underlying chromospheric gas, which may be able to explain the ceaseless dynamics observed in the transition region (e.g., Brueckner et al. 1983; Mariska 1992); Judge et al. 1997), but probably cannot explain spicules. Of course the details of the actual geometry of spicule magnetic fields and the form of the radiation losses in spicules are unknown, and so they may not be correctly incorporated in the model. Fortunately, this rebound shock model makes a testable prediction: The motion of the tops of spicules should be non-steady both during its upward evolution, and during its return to the solar surface (Cheng 1992c; Hansteen et al. 1994), since the rebound shocks only intermittently strike (and hence accelerate upward) the transition region. So far, the data are uncertain in this regard; some observers (e.g., Lippincott 1957; Zirker 1967; Weart 1970; Tsiropoula et al. 1994) have noted velocity variations in spicules or spicule-like disk features, but Suematsu et al. (1995) report that there is no evidence at all of periodic acceleration in spicule-like disk features. We will have to wait to see if higher spatial- and temporal-resolution observations will clarify this issue.

As with the strong-pulse model, Sterling et al. (1988) found the rebound shock model results in lower-height spicules as the initial transition region height is reduced; the reason is likely to be the same as that described by Shibata et al. (1982a) discussed above. Sterling et al. (1990), however, found that the effect was not very pronounced when radiation losses were included, because the strength of the shocks was limited more by the strong effects of radiation losses than by the initial height of the transition region.

3.3 Pressure Pulse in the Higher Chromosphere

This scenario, which assumes that a burst of energy in the form of a pressure pulse is released higher in the chromosphere than the previous models, also results in chromospheric ejections. This concept is similar to solar flare simulations resulting in “chromospheric evaporation,” due to particle beams deposited in the upper chromosphere (e.g., Nagai et al. 1984), except the amount and rate of energy input is much less in this case. (This is different, however, from flare models based on conduction due to an energy deposition in the corona, e.g. Nagai 1980, since we require the bulk of the energy to be deposited directly somewhere in the middle of the chromosphere, rather than at the very top of the chromosphere.) Thus these models are consistent with suggestions that small flares or microflares might be the source of spicules or other jet-like eruptions.

Shibata et al. (1982b) examined this possibility in an attempt to explain surges, where radiation and heat conduction were not included. They found that the sudden energy deposition can lead to two different phenomena: First, it causes an expansion of the nearby plasma along the flux tube as the pressure pulse expands, and second, this expansion can generate a shock wave. Based on these results, they defined two types of chromospheric jets, with the difference being what causes the transition region to be pushed upward. In one case, the transition region is directly expelled by the expanding pressure pulse; they refer

to this type of jet as a “shock tube” jet. In the other case, the transition region is ejected by the slow shock wave generated by the pressure pulse; they refer to the resulting jet as a “crest shock” jet. They found that the type of jet produced depends on the height of the energy deposition in the chromosphere. Above some critical height (located in the middle chromosphere), only the shock tube jet forms, and below that height, only the crest shock jet results. Shibata (1983) discusses basic physics issues regarding simulations of pressure releases in various regions of the lower solar atmosphere.

Steinolfson et al. (1979) had performed a similar type of study, with which they matched some observational properties of surges. They only considered energy releases in the upper part of the chromosphere, and therefore did not find the two types of solutions discovered by Shibata et al. (1982b).

Sterling et al. (1991) and Sterling et al. (1993) added the effects of radiation and heat conduction in a series of similar calculations, and they did produce a spicule model from a subset of their calculations. Sterling et al. (1993) used an open magnetic field coronal hole (or very large quiet region loop) setup, and deposited energy at various heights in the middle and upper chromosphere. They were able to recover the two types of jets of the above Shibata et al. (1982b) and Shibata (1982) studies, with some modifications in properties because they allowed more freedom in selecting the initial energy source parameters. Sterling et al. (1993) also identified different types of structures, which they referred to as “pressure-gradient” jets, which are jets associated with the expanding pressure pulse in the chromosphere (these are similar to the shock tube jets of Shibata et al. 1982b); two-component jets, which have a pressure-gradient part below a shock-generated part (these are identical to the “crest-shock” jets of Shibata et al. 1982b); and “gas plugs,” which are packets of chromospheric material detached from the chromosphere and ejected out into the corona at high velocities ($\sim 100 \text{ km s}^{-1}$). It is some of these pressure-gradient jets of Sterling et al. (1993) that resemble spicules in dynamic and thermodynamic properties.

Figure 3a and 3b illustrate the model spicule solutions of Sterling et al. (1993). In this case, the flux tube expands with height in the chromosphere. But since the principal dynamics occurs above the heights where the expansion is greatest, calculations using a constant cross section (Shibata et al.—1982b; Shibata 1982; Sterling et al. 1991) should not differ much from those using a varying cross section geometry. Usually the spicules form when the uppermost 500-1000 km (where the top of the chromosphere is at about 2000 km) of the chromosphere receives the bulk of the input heating. This heated region expands, as shown in Figure 3b, to spicule heights. Because the pressure force associated with the input energy source counteracts gravity in Equation 2, the motion of the model spicules in Sterling et al. (1993) is different from ballistic, with spicule heights being achieved with initial velocities less than those required for ballistic motion. Also, the motion of the top of the model spicule is smooth.

This model also has a computational advantage over those with a lower-height energy source in that it is not as critically dependent on difficult-to-calculate details of radiation losses in the lower chromosphere. For example, the most extreme of the lower-atmospheric radiation losses occur near the photosphere (e.g., Gibson 1973; Giovanelli 1978); none of the models discussed in §3.2 have fully considered these effects.

This model predicts a brightening in the chromosphere before or coincident with the spicule’s formation. This, however, is at odds with observations of disk features by Suematsu et al. (1995), who find that such brightenings occur *after* the features are formed. This

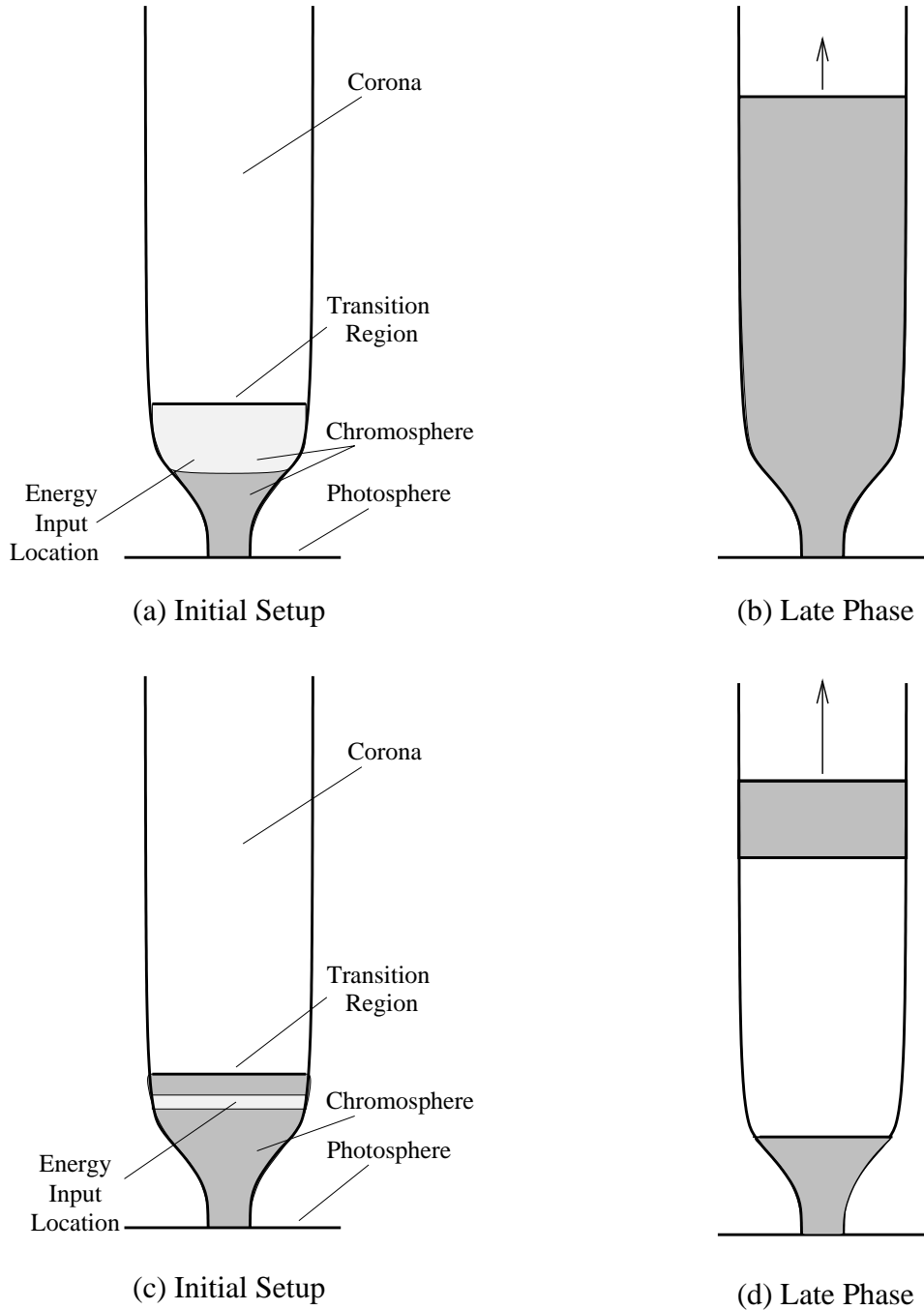


Figure 3: Schematic diagram of a model spicule produced by a pressure pulse in the middle chromosphere (top two panels). The initial setup is as in Fig. 2a. Here, the middle and upper portion of the chromosphere undergoes heating, indicated by the light-grey region. This heated region expands and cools in later phases, resulting in a spicule-like structure for selected input parameters. The bottom two panels show what happens for a different set of input parameters, whereby the input energy region is restricted to a very narrow region. In late phases, a “gas plug” of cool chromospheric material is ejected out into the corona, with corona both above and below the elevated gas plug. This feature does not represent a spicule, but material below the ejected gas plug may appear as an X-ray jet.

difficulty, incidentally, also plagues the spicules simulated by Suematsu et al. (1982). Porter et al. (1987) and Fontenla et al. (1989) suggested that UV microflare brightenings seen in the network may be responsible for spicules. Sterling et al. (1993) predict brightenings in excess of 100,000 K, and therefore expected to appear in some UV and EUV lines, for a subset of their parameter space which leads to spicule solutions. But the majority of the cases that lead to spicules are suspected to be associated with H α brightenings (based on temperature and density profiles; no radiative transfer calculations were actually performed), but *not* with such UV brightenings.

If this model is valid, then one would expect that at times the form of the heating source would be different from those that result in spicule solutions. In particular, Figures 3c and 3d illustrate a case in which a gas plug forms. Here, the heating is localized to a narrow region below the transition region. If the energy level is above a threshold level (a heating rate large enough to heat the chromospheric material at the input location to coronal temperatures), the chromosphere above the energy input location is expelled into the corona as a gas plug, while the heated region itself transforms into coronal material. (Physically, after material of this directly-heated region reaches a temperature of about $10^{5.4}$ K, it becomes radiatively unstable and a new equilibrium is reached with coronal conditions; see Sterling et al. 1993.) This heated material below the gas plug is enhanced in density, and may appear as an X-ray jet such as those seen with the *Yohkoh* Soft X-ray Telescope (SXT) (see §5.6). The gas plugs themselves would appear as clumps of detached chromospheric material being ejected away from the Sun. When the energy input rate is large enough the gas plug can evaporate while moving through the corona.

Sterling et al. (1991) used a quiet region magnetic flux loop setup and restricted the energy deposition to the upper portion of the chromosphere. They found only gas plug or evaporating gas plug solutions in this circumstance; in particular, they found no spicule solutions.

3.4 Alfvén Waves

We divide this discussion into two groups, one depending primarily on lower-frequency Alfvén waves, and a second from a recent set of studies—based on a different Alfvén-wave mechanism—which depends upon higher-frequency Alfvén waves.

3.4.1 Low-Frequency Alfvén Waves

All of the simulations discussed so far have been purely hydrodynamic. There have also been a series of MHD spicule simulations where the driving mechanism is suggested to be torsional Alfvén waves on vertical flux tubes, that is, axisymmetric twists on vertical flux tubes in the azimuthal direction. This is an appealing suggestion, since Alfvén waves may be a natural result of buffeting of magnetic flux tubes by photospheric granulation. Also, there have been suggestions that spicules (e.g., Livshits 1967; Pasachoff et al. 1968) and UV spicules (Cook et al. 1984) undergo twisting motions as they evolve, which propagating torsional Alfvén waves could possibly explain.

Hollweg et al. (1982) did the first detailed set of simulations in this class, using an initial setup similar to that shown in Figure 2a. These are sometimes described as “1.5-d” simulations, in which motions in the vertical (z) direction and the azimuthal directions are allowed, but motions in other directions are suppressed. They showed that the Alfvén waves can

non-linearly couple into MHD fast-mode shocks, which can move the transition region and chromospheric material below it upward. Hollweg (1992) continued these studies by considering the role of an MHD slow-mode shock that is also produced as a result of the non-linear evolution of the Alfvén wave.

Even though those studies did not include radiation losses, it was already difficult to reproduce a convincing spicule. In the Hollweg et al. (1982) work, for example, the uplifted chromospheric material was too cold for spicules due to adiabatic expansion of the material. The slow shocks of Hollweg (1992) produced structures which were of insufficient height, and maybe still too cool to be regarded as spicules, although the temperatures may just reach the lower end of the reported range of observations.

Mariska et al. (1985) found that incorporating radiation losses in similar calculations results in a further reduction of height in the structures. That study, however, assumed an initial atmosphere representative of an active region loop, rather than a quiet region structure. As noted earlier, work of Shibata et al. (1982a) and Sterling et al. (1988) indicate that tall spicules might not be expected when the transition region is at a reduced height (as is the case in modeling active regions). Nonetheless, the above-noted adiabatic Alfvén wave model calculations of Hollweg et al. (1982) and Hollweg (1992), which did assume an initial atmosphere closer to quiet-region or coronal-hole conditions, also failed to produce a satisfactory spicule.

Cargill et al. (1997) performed a similar calculation in a two-dimensional geometry, but without radiation and heat conduction. Their calculations once again resulted in ejections of chromospheric material into the corona which were too short to represent spicules.

All of the above calculations concentrate on the evolution of a single Alfvénic pulse on a flux tube. Kudoh et al. (1999) have extended this model by using a series of random Alfvénic pulses, but not including radiation losses or heat conduction. Their resulting model spicule reaches about 5000 km, with temperatures of 6000–10,000 K, although radiation losses would probably lower these heights (cf. Mariska et al. 1985) and alter the temperatures. Hollweg et al. (1982) and Kudoh et al. (1999) suggest that the Alfvén wave flux is large enough to explain heating of the quiet corona and non-thermal line broadenings. Moreover, Kudoh et al. (1999) show that the non-thermal fluctuation as a function of temperature predicted by their calculations are in general agreement with observations of line broadenings in the transition region.

Spicules of the nature described here also appear as a by-product of the 2.5-dimensional resonance absorption study by Belien et al. (1999). An interesting point of their spicule-like features is that, even though the Alfvén wave excitation takes place at only one end of a coronal loop, spicules are created at both ends of the loop, and both seem to reach similar heights. The mechanism for the production of the spicule at the far-end of the loop was not elucidated in their paper, which was primarily concerned with the question of coronal heating.

3.4.2 High-Frequency Alfvén Waves

Haerendel (1992) and dePontieu et al. (1998) introduce a spicule model, using an analytical analysis, based on high frequency inputs (periods of about 1 to 5 s), where the operative mechanism is Alfvén wave damping by ion-neutral collisions. This contrasts with the above Alfvén-wave models which, except for the Kudoh et al. (1999) work, were restricted to low-frequency input Alfvénic disturbances of 30–60 s. (Kudoh et al. 1999, include both low

and high-frequencies in their calculations, but the dynamics they describe are similar to the other low-frequency Alfvén wave simulations; they did not consider the possibility of ion-neutral damping in their work.) According to this Alfvén wave damping model, a train of Alfvén waves generated in the lower chromosphere is damped by collisions between ions and neutrals as it travels upward through the partially-ionized middle chromosphere. This type of damping results in a net upward-directed $\mathbf{J} \times \mathbf{B}$ force on the plasma which drives the spicule, and the damping also heats the plasma (Piddington 1956).

This model requires that an energy flux of $10^6 \text{ erg cm}^{-2} \text{ s}^{-1}$ be injected in Alfvén waves with frequencies roughly between 0.2 and 0.6 Hz, although the actual range depends upon the parameters used. Frequencies higher than this limit would result in damping over too short a distance to produce spicules of sufficient height, while frequencies lower than this range would require excessively large wave amplitudes. This amplitude limit would be set by velocities (spectral line broadenings) observed in the photosphere at the base of the flux tubes. Although there is certainly the required level of flux available over the entire range of photospheric motions (since coronal heating requires this level of flux), it is not known whether this amount of flux is available in Alfvén waves over the restricted frequency range required by the model.

While dePontieu et al. (1998) showed that the damping can provide enough momentum and energy to support and heat an already existing spicule, dePontieu (1999) performed numerical simulations based on this mechanism. Those simulations were done in the WKB limit, that is, assuming that the changes in the background atmosphere are not great over the distance of a wavelength. He includes wavelength-averaged expressions for the energy term and momentum terms due to the calculated damping mechanism. These terms are added to Equations (2) and (3), via appropriate forms for F and E . In this way dePontieu (1999) sets up a set of hydrodynamic equations (including Equations 1—4) which approximately describes the effects of the high-frequency Alfvén waves in the chromosphere; thus he effectively approximates the effects of the Alfvén waves in the calculation, without having to explicitly consider the magnetic field. This system is solved, including expressions for optically-thin radiation losses and ionization effects, but not heat conduction. The resulting calculations do indicate that this model can explain basic spicule properties. He found, for example, that a continuous input source of magnitude 2.5 km s^{-1} at a height of 250 km above the photosphere results in a spicule-like structure with flat temperature and density profiles, reaching heights of about 5000 km with temperature of about 6,000—8,000 K, and upward velocities near 20 km s^{-1} . A source that turns off after 300 s (about the lifetime for the rise of a spicule) yields similar results.

As with the other models, there are still outstanding points to be addressed with this suggested mechanism. In addition to the question noted above of the requirements for the Alfvén wave flux over a restricted frequency range, the studies make use of a number of approximations, including restricting the analysis to the WKB limit. Thus one improvement would be to move toward self-consistently solving the MHD equations for this system, admittedly a computationally challenging problem to solve in full if physical effects such as radiation losses and ionization are included. It is not clear whether these refinements will impede or enhance spicule generation.

4 Other Models

There have been several analytical models and other suggested mechanisms for spicule generation. Most of these were developed before the computational era got fully underway. In addition, there are numerical models for features not initially aimed at explaining spicules, but which could conceivably be applicable to spicules also.

Since the review of Beckers (1972), but before the era of numerical simulations, Unno et al. (1974) considered an analytical model of spicules which described them as similar to geysers. They suggest that magnetic buoyancy could provide an initial flow at the foot of a spicule, and that this can be enhanced by acoustic waves. Based upon this type of flow model, Pampushev (1980) briefly discusses the expected maximum heights of spicules based on pressure balance arguments, and Schatten et al. (1986) discuss a similar mechanism. Simulations of Steiner et al. (1998) may be applicable to the granular buffeting of flux tubes discussed by, e.g., Roberts (1979), although they do not extend their calculation region far enough into the chromosphere and corona to directly examine spicules.

Hollweg (1972) suggested that spicules could result from sheets of plasma being compressed by magnetic fields, with the spicule expelled upward. Hasan et al. (1981), however, find that this mechanism would require the magnetic fields to be driven together with a rather high velocity ($\gtrsim 60 \text{ km s}^{-1}$) in order to generate a spicule; they suggest that thermal collapse (Thomas et al. 1961) may provide a possible trigger for the mechanism.

Roberts et al. (1982) suggested that solitons may be generated in intense photospheric flux tubes and be manifest as spicules in the chromosphere. This is an interesting suggestion for a source for spicules, but their analysis only deals with the solitons themselves. Velli et al. (1999) consider the generation of Alfvén waves by vortex sinks in the photosphere and by reconnection. Somewhat more generally, Solanki (1998) discusses possibilities for the photospheric sources of various jets in the solar atmosphere.

Hirayama (1992) suggested that spicules may be a byproduct of joule heating in the current sheet forming the boundary of slender photospheric magnetic flux tubes. He calculates the joule heating in such flux tubes to be of order $10^9 \text{ erg cm}^{-2} \text{ s}^{-1}$, and so a flux tube of 150 km diameter undergoing such heating over the duration of 1 min would have energy output comparable to the gravitational energy of a spicule (§2). Lorrain et al. (1996) have also proposed an electromagnetic mechanism for spicule generation, whereby a self-excited dynamo drives a proton beam via a $\mathbf{v} \times \mathbf{B}$ force. Henoux et al. (1997) also investigate an electromagnetic driving mechanism, taking into account a three fluid plasma (electron, ions, and neutrals). These ideas have yet to be explored with numerical simulations to see if spicule-like properties result.

Magnetic reconnection continues to receive attention as the ultimate source for driving spicules. Sterling et al. (1991) and Sterling et al. (1993) suggested that magnetic reconnection may be a source for energy depositions in the middle and upper chromosphere, possibly leading to spicules. Karpen et al. (1995) have made an initial attempt to understand a variety of chromospheric eruptions resulting from reconnection using 2.5-dimensional simulations. Andreev (1996) and Yokoyama et al. (1995, 1996) also report on findings based on reconnection in the chromosphere and ejection of chromospheric material. There is some observational evidence for the energy releases in the transition region resulting from reconnection (e.g., Tarbell et al. 1999), while transition region brightenings have been related to the magnetic network regions of the Sun for some time (e.g., Porter et al. 1987). Pataraya et al. (1990) analytically calculate the expected rate of development of flux tubes at the supergranule

boundaries, and speculate that spicules result from the formation and coalescence of these flux tubes via an unstated process.

Another type of magnetic mechanism has been suggested by Moore et al. (1999). They take the view that eruptive flares result when a highly sheared “core” magnetic field destabilizes and erupts, and that spicules are miniature flares. Thus each spicule would consist of a bipolar magnetic element, perhaps with an overlying restraining magnetic arcade, at its root. Eruption of the core field would eject material trapped in the surrounding fields upward, channeled along vertical magnetic flux tubes. Observations by Wang et al. (2000) argue that such eruptions are distinct from macrospicules; macrospicules may or may not be similar to spicules. See §5.4.

Tsirul’nik (1984) and Shibata et al. (1986) have numerically investigated the generation of chromospheric jets and other features via untwisting of magnetic flux tubes. As mentioned earlier, there are some suggestions that spicules do spin, and so these mechanisms may be adaptable to the spicule problem.

It has been suggested that spicules are driven by thermal conduction from the corona (e.g., Kuperus et al. 1967, Kopp et al. 1968, Moore et al. 1972), or by an interruption in coronal heating (Athay 1984), which is worth considering since the energy flux required for spicules and for quiet coronal heating is similar in magnitude. Rabin et al. (1980), however, point out that the conductive flux in coronal holes is several times less than that outside of coronal holes, but that the properties of spicules inside and outside coronal holes do not differ greatly, indicating that conduction is not the source for spicules. Since spicules inside coronal holes are, in fact, slightly taller than those outside coronal holes (which they also present observational evidence for in the same paper), they note that back conduction, if anything, reduces the height of the spicules. (Rabin et al. 1980), however, also note that the values they use for conduction are based on hydrostatic models with simple field geometry which does not account for spicule-like structures; therefore their findings are suggestive, but perhaps not definitive.) As pointed out earlier, if the ambient (non-spicule) transition region outside of coronal holes is at a lower height than that inside of coronal holes, Shibata et al. (1982a) and Sterling et al. 1988) have shown that the respective models they study result in reduced-height spicules outside the coronal holes. This is in accord with the Rabin et al. (1980) observations.

In preliminary work Suematsu (1990) and Suematsu et al. (1991) have examined the possibility that the 5-minute oscillations can drive chromospheric motions. The acoustic waves that are the source of the 5-minute oscillations are evanescent for vertical fields, and consequently little chromospheric motion is induced in that case. For low-beta field lines inclined $\gtrsim 50^\circ$, however, it may be possible to induce chromospheric motions along the field lines.

5 Spicule-Like Features

I have only addressed chromospheric spicules in detail in this paper. There are also a number of spicule-like features occurring in the solar atmosphere, which may or may not be related to spicules themselves. Here I briefly discuss these features in terms of the spicule models described above.

5.1 Mottles

As discussed in the spicule reviews cited in §2, the disk representation of spicules is an issue of ongoing debate, but they are most frequently assumed to be associated with the “dark mottles.” (Bhavilai 1965, associated them with the “bright mottles,” but the idea does not seem to have been pursued; see discussion in Athay 1976.) In addition to the reviews in §2, Bray (1969), Tanaka (1974), Gaizauskas (1985), Cram (1985), Zirin (1988), and Foukal (1990) also review disk features. Gaizauskas (1984) corroborated that these features are related to spicules by noting that a cluster of spicules at the limb appeared as a cluster of elongated dark mottles on the disk a day later (of course, individual spicules could not be identified with individual mottles since the lifetime of either feature is only a few minutes). Nonetheless, it is possible that spicules and mottles are independent structures (e.g., Grossmann-Doerth et al 1992).

None of the above models explicitly differentiate between spicules and mottles, but Sterling et al. (1993) note that their two-component jets could correspond to some reports that mottles are bright near their base and darker further away (e.g., Athay 1976; Foukal 1971; Foukal 1990). Although some observations suggest that the bright mottles and dark mottles are two distinct features (e.g., Heinzel et al. 1994), other observations suggest that they could sometimes be different portions of the same jet feature (Beckers 1968, 1972). In the latter case, the bright portion could correspond to the pressure-pulse driven lower part of the two-component jet, which is hotter than the shock-driven upper portion of the jet. Sterling et al. (1993) did not calculate expected $H\alpha$ emission signatures for these features, however, and therefore these comments are purely speculative. Moreover, Bray (1969) argues against the two types of mottles being part of the same feature.

5.2 Fibrils

Fibrils appear to be spicules (or, more precisely, mottles) that are low-lying and have a horizontal orientation (e.g., Zirin 1988; Foukal 1990; reviews cited in §2). Thus a mechanism acting on a vertical field which produces spicules might be expected to produce fibrils on more horizontal fields. Suematsu (1985) applied the strong pulse mechanism of §3.1 to a low-lying coronal loop in an effort to reproduce fibrils. Similarly, Sterling et al. (1989) applied the rebound shock model to a magnetic field with a horizontal component in order to model solar fibrils. Both studies resulted in fibril-like solutions, although neither study incorporated radiation losses.

5.3 UV and EUV Spicules

Spicule-like features are also seen at UV and EUV wavelengths (Bonnet et al. 1980; Dere et al. 1983; Withbroe 1983; Cook et al. 1984; Brueckner et al. 1986; Dere et al. 1989; Cook 1991; Karovska et al. 1994a). Whether these features are the same as the chromospheric spicules has not been established. Observations of Karovska et al. (1994a) suggest that they may be identical, but Mariska (1992) points out some of the difficulties in establishing this identification. None of the numerical models examined above produce spicules hot enough to appear in UV, with the possible exception of simulations such as those in Sterling et al. (1993) which may result in UV microflares (or very short UV spicules) in some circumstances. Some of the gas plug solutions of Sterling et al. (1993) may result in emission in EUV or X-rays. It is possible that UV or EUV jets are standard spicules heated to high

temperatures by an ongoing energizing process (e.g., Pneuman et al. 1978; Poletto 1980; Athay et al. 1982; Sterling et al. 1984; Sterling 1998b). Budnik et al. (1998) interpret their observations of spicule-like features between 3×10^4 and 6×10^5 K as showing such evaporation, but their observations also seem to be consistent with a spicule “sheath,” where the width and height of the sheath increase with temperature.

Two attractive features of the suggestion that spicules may be heated before they fall is that it may explain (a) why many spicules seem to fade from $H\alpha$ after reaching their maximum height, and (b) such heated, falling spicule material could explain the pervasive redshifts seen in UV (e.g., Pneuman et al. 1978; Poletto 1981; Mariska 1992; Gallagher et al. 1999). As mentioned earlier, Hansteen et al. (1994) have calculated the expected spectral signatures of the transition region as it falls in the rebound shock model for spicules. They found that the apparent signature would be perceived as an upflow rather than a downflow, due to the way in which the density and velocity are correlated in the version of the model that they adopt. Those calculations, however, refer to the motion of the transition region at the top of the model spicule; the bulk of the model spicule itself would remain cool ($T \lesssim 10^4$ K) without an additional heating source. The expected spectral signature for a model spicule after it has been heated to UV-emitting temperatures (i.e., after it has “evaporated” out of visibility in $H\alpha$) would depend upon the nature of the heating mechanism.

In addition to the spicule-like UV features, there are a variety of other transition region energetic events that may be related somehow to spicules. Mariska (1992) summarizes observations of these events.

Cook (1991) also discusses UV features he refers to as “superspicules,” which are longer, fainter, and much less common than the (typical) UV spicules. Very little is known about these features.

5.4 Macrospicules

Macrospicules are jets or small surge-like features of size scales larger than spicules. They extend from about 7,000—40,000 km above the limb with lifetimes of 3—45 minutes (Dere et al. 1989; Karovska et al. 1994b). They are visible in EUV (e.g., Bohlin et al. 1975; Withbroe et al. 1976; Dere et al. 1989), as well as in $H\alpha$ (e.g., Moore et al. 1977; LaBonte 1979; Loucif 1994; and Karovska et al. 1994b, who discuss much earlier $H\alpha$ observations), and in radio (Habbal et al. 91), and they are concentrated in the polar coronal holes.

Although macrospicules are so named because they appear to be giant spicules, there is no certainty that they are actually related to spicules. For example, Wang’s (1998) observations suggest that EUV macrospicules (seen in He II) follow a different size distribution from spicules. Thus it may not be necessary to require that a spicule model also be able to explain surges or macrospicules. Macrospicules may be different from surges too, as Georgakilas et al. (1999) point out that these two features also appear to differ in their physical properties. Moore et al. (1977) and LaBonte (1979) classified miniature filament eruptions as one form of macrospicules, whereas Wang et al. (2000) present evidence that miniature filament eruptions and macrospicules are two different forms of activity. Part of the discrepancy may be due to semantics of the definition of macrospicule.

Shibata (1982) suggests that the “shock tube jets” and the “crest shock jets” of Shibata et al. (1982b) can correspond to $H\alpha$ macrospicules and to EUV macrospicules not seen in $H\alpha$, respectively. His argument is based on the density of the former type of jet being higher than that of the latter. It is not clear, however, what would heat the crest shock jets to

EUV-emitting temperatures, since adiabatic expansion below the crest shock leads to cooling of the ejected material in the simulations.

Pike et al. (1998) discuss rotating motions of macrospicules seen in EUV from the CDS instrument on *SOHO*; they refer to these features as “a sort of solar tornado.” The presence of twisting motions may indicate the existence of Alfvén waves on these structures. If the Alfvén waves exist on a resonance cavity formed on the macrospicule, then periodicities in the velocity amplitudes of the twists would be expected (Sterling 1998b). In practice, it is difficult to interpret the Pike and Mason results regarding the existence of oscillations, and more careful analysis would be needed for a definitive answer (C. D. Pike 1998, private communication). Moreover, the theory discussed in Sterling (1998b) is only approximate; it assumes a constant-length spicule, for example. As with surges, the winding (Tsirul’nik 1984), or unwinding (Shibata et al. 1986) of magnetic flux tubes may also explain the observed twisting motions, and the analysis of slow twists by Hollweg et al. (1989) in their “close to the Sun” limit may also be applicable.

5.5 Surges

Some workers have suggested that both spicules and surges (e.g., Roy 1973; Rust et al. 1980; Zirin 1988) have a common driving mechanism, only differing in scale or input parameters (e.g., Blake et al. 85), with surges being much larger than spicules. Some recent observations, however, indicate that surges are different from spicules. Suematsu et al. (1995) find that spicule-like features on the disk do not generally have brightenings at their bases until after the feature is already extended. In contrast, they note that surges start with a small flare at their base. Also, whereas surges are associated with cancelation of magnetic flux (e.g., Gaizauskas 1996), spicule-like features appear to emanate from unipolar regions (Suematsu et al. 1995).

Steinolfson et al. (1979), Shibata et al. (1982b) and Sterling et al. (1993) found numerical results that may correspond to surges. Sterling et al. (1993) found that these types of simulations based on pressure pulses in the higher chromosphere could not produce extended $H\alpha$ features (spicules or surges) coincident with a strong soft X-ray signature at the base. Observations, however, show that surges are often accompanied by soft X-ray features (e.g., Schmieder et al. 1988; Shibata et al. 1992; Schmieder et al. 1995; Schmieder et al. 1996; Canfield et al. 1996). Such observations therefore seem to rule out a pressure pulse origin for surges according to Shibata et al. (1992). This is not definitive, however, since the accompanying X-ray loops or X-ray jets are generally offset to one side of the $H\alpha$ surges (e.g., Canfield et al. 1996), and so it could be that the actual root of the surge receives a level of heating too low to emit in X-rays, but large enough to cause a pressure-pulse surge that does not evaporate. Directly above the low-altitude X-ray brightening (and located adjacent to the root of the surge), an X-ray jet may appear, but not an $H\alpha$ surge. This would be consistent with the findings of Sterling et al. (1993, 1994). A difficulty with the Sterling et al. (1993) work regarding surges, however, is that they were not able to produce features taller than about 30,000 km, although this may be a result of parameter selection. Surges can reach heights of 20,000—200,000 km.

An alternative explanation was suggested by Shibata et al. (1992), whereby the X-ray jet results from heating due to reconnection and the surge results from a dynamic whip-like movement of newly-released magnetic fields. This idea has been explored using 2-dimensional simulations by, e.g., Yokoyama et al. (1995, 1996). Observations mentioned above of surges

adjacent to X-ray jets by Canfield et al. (1996) are consistent with predictions of such a 2-dimensional, whip-like motion scenario.

5.6 X-Ray Jets

These are features discovered with the *Yohkoh* SXT (Shibata et al. 1992, 1994); Strong et al. 1992). Shimojo et al. (1996) summarize their properties, noting that they have average lengths of 1.5×10^5 km, apparent projected velocities from 10 km s^{-1} to about 1000 km s^{-1} , lifetimes from 100 s to 16,000 s, and are often associated with small flares at their footpoints. Other aspects of X-ray jets are discussed by, e.g., Canfield et al. (1996) and Kundu et al. 1995, 1998, 1999). Reconnection could be responsible for depositing the energy at the base of the jet (e.g., Shibata et al. 1992; Yokoyama et al. 1995, 1996). In a preliminary investigation, Sterling et al. (1994) suggest that X-ray jets could result from the deposition of energy in the higher chromosphere in cases where a gas plug or evaporating gas plug of Sterling et al. (1991, 1993) is ejected. The material below the ejected gas plug is enhanced due to evaporation of chromospheric material, and heated due to the energy input, and therefore will have an enhanced intensity that could appear as an X-ray jet (cf. §3.3).

6 The State of Our Understanding

Over the past two decades, numerical simulations have augmented theoretical concepts for producing solar spicules by showing that, in many cases, the atmospheric response is roughly in accord with observations, such as approximately constant (compared to hydrostatic equilibrium) density and temperature along the spicule length. Nonetheless, it has been difficult to satisfactorily reproduce the key properties of spicules using what seems to be the most appropriate set of input parameters. That is, in many cases examined, numerical simulations do not reproduce the most-often-quoted values for temperatures, densities, upward velocities, perhaps non-ballistic behavior, and lifetimes of spicules, when radiation, heat conduction, and magnetic field expansion are all included in the expected fashion. In other cases, e.g., the pressure-pulse in the higher chromosphere, the simulations can match spicule observations in many aspects, but there is no obvious reason for the spicule-producing input parameters to be favored over the non-spicule-producing input parameters.

There are several possible reasons for the lack of better match between theory and observation. One such factor is that the “most-often-quoted” values for spicule parameters may not be the “most-often-correct” values. As noted in §2, spicules are near the limit of resolution for ground-based instruments, and so some of the values obtained so far are contradictory, and others are open to question. Compounding the difficulty is that it is still not certain what disk features correspond to limb spicules. Grossmann-Doerth et al. (1992) illustrate how poor our state of knowledge of the observational properties of spicules is by demonstrating that we still cannot reconcile differences in the observed velocities of spicules at the limb and their often-presumed manifestation on the disk as dark mottles. Dere et al. (1983) go even further, making a respectable argument that the dark mottles are not related to spicules at all. Furthermore, it is not certain that apparent motions seen at the limb are all due to mass motions, rather than to waves of excitation.

Another factor is that the approximations and assumptions of the models may be inadequate or incorrect. The solar atmosphere is certainly much more complicated than assumed in the models (e.g., Feldman 1983). Just how reasonable or unreasonable the assumptions

in the simulations are in regard to spicule formation is not easy to ascertain. Again, the observations are not complete enough to make this determination.

Yet another factor is that not all of the above simulations have been evaluated under the “most appropriate” circumstances. Effects such as radiation losses, heat conduction, ionization, magnetic field geometry, non-rigid magnetic field, etc., will have to be incorporated into models in a consistent fashion before the most meaningful comparisons with observations (and among the models themselves, for that matter) can be made.

Each of the numerical models discussed in this review have distinctive features that can be compared with observations, and some models require further development computationally. For example:

- Strong pulse model. Predicts smoothly rising, ballistic velocity profiles with initial velocities of $\approx 60 \text{ km s}^{-1}$ (for the top of the spicule). Also predicts bright points at the base of spicules at onset, and cool temperatures for spicules. Future development of this model should examine the effects of loss mechanisms and flux tube cross-sectional variation.
- Rebound Shock Model. Predicts non-ballistic intermittent rise of velocity profile and does not require high ($\approx 60 \text{ km s}^{-1}$) ballistic initial velocities. No bright point required at the base of the spicule. Simulations including loss mechanisms struggle to produce spicules of adequate heights, velocities, and temperatures. It would be useful to study this idea using higher-dimensional and MHD (as opposed to assuming a rigid magnetic field) codes to see if the interaction of the magnetic field with the plasma can increase the energy contained in the upward flows.
- Pulse in the higher chromosphere model. Predicts smooth velocity profiles and a velocity profile closer to constant than required for ballistic motion. Does not require high ($\approx 60 \text{ km s}^{-1}$) onset velocities. Predicts bright point at the base at spicule onset. Spicule-like features are only a subset of the solution space using reasonable input parameters; therefore one expects observations of auxiliary phenomena corresponding to gas plugs, denser spicules, etc., depending upon input parameters.
- Alfvén-wave models. Could explain suspected twisting motions on spicules, and perhaps heating of the quiet corona. Alfvén waves are seen in the solar wind (e.g., Belcher et al. 1971), so we know they do exist at some level in the solar context. The work of Mariska et al. 1985), where radiation losses and heat conduction are included, should be extended to cover a wider range of input parameters, e.g., corresponding to quiet regions. Even models without loss mechanisms struggle to produce spicules of adequate heights, velocities, and temperatures when the input force corresponds to velocities $\approx 1 \text{ km s}^{-1}$.

Spicules generated with the Alfvén wave ion-neutral damping model in the initial simulations by dePontieu et al (1999) were of lower height than observed spicules, but this might be remediable by exploring a wider parameter space. Also, further investigations using MHD analysis and examining the non-WKB-limit regime will be interesting. Observations will have to show whether the amount of energy flux at the high frequencies required by the idea is present.

In addition to further development of existing numerical spicule models, new theoretical ideas can be explored in depth by trying to model some of the energy sources suggested in §4.

New observations may, of course, suggest that hitherto untried approaches to spicule models are more appropriate. Since the magnetic field is clearly related to spicule existence, it would be useful to consider new magnetic field-based models. Moreover, exploration of such models will certainly tell us much about physics of the solar atmosphere, independent of whether such mechanisms lead to spicules.

A particularly sobering point is that recent numerical and observational studies of Carlsson et al. (1995, 1997a, 1997b), providing evidence that a 10,000 K chromosphere may not actually exist in non-magnetized regions. Instead, complex dynamics occurring in those regions may masquerade as a static, warm chromosphere, with the chromospheric high temperatures existing only intermittently in association with propagating acoustic shocks. Their results are based on comparisons of observations with output from a numerical simulation which self-consistently treats radiation and hydrodynamics. Carlsson et al. (1995) find that viscous dissipation of acoustic shocks is balanced by radiative cooling, resulting in no increase in temperature in the chromosphere. Infrared observations of CO lines by Solanki et al. (1996) are supportive of a pervasively cool chromosphere. As Carlsson et al. (1997b) note: “The implications of this new development, if it survives further critical analysis, are far reaching.” If their suspicions hold for the magnetized network regions also, these far-reaching implications will extend to all of the spicule models we have discussed here, since they all assume an initially steady, 10^4 K chromosphere.

7 Targets for Future Observations

Finally, here are some specific questions that have to be clarified observationally before we can fully address the challenge of explaining spicule production theoretically:

- What are the velocities of spicules? Are the rise velocity profiles ballistic, which favors, e.g., the strong pulse model, or are they more-constant-than-ballistic, as predicted by the rebound-shock model or model with a pulse in the middle or upper chromosphere?
- Do spicules rise with a smooth velocity profile, or do they rise intermittently “in jerks [Lippincott 1957]”? Rush et al. (1954), Lippincott (1957), Bray et al. (1974), and Suematsu et al. (1995), among others, discuss observations related to this point for spicules and related disk features. This issue is important in distinguishing between mechanisms such as the rebound shock model—which predict an intermittent rise during the primary spicule evolution—and mechanisms such as the strong pulse model or the model with the pressure pulse in the higher chromosphere, which predict a smooth rise trajectory.
- What are the temperatures of spicules? Do they require substantial heating during their rise to produce temperatures of about 12,000—16,000 K (e.g., Beckers 1968, Beckers 1972; Cuny 1987), or are they substantially cooler (e.g. Nikol’skii et al. 1967 and references therein; Landman 1984; Matsuno et al. 1988; Braun et al. 1987)? This information will help to determine how much heating is needed in spicules as they rise.
- What are the radiation losses in spicules? This is a key question for refining any spicule model.
- What are the disk manifestations of spicules? This is a long-standing question which still awaits a satisfactory answer (e.g., Grossmann-Doerth et al. 1992).

- What are the true heights of spicules, taking into account the fact that they appear to be suspended above the photosphere (e.g., Loughhead 1969; Nikolsky 1970; Gaizauskas 1984)? Their “suspension height” can be understood if the source is in the middle or upper chromosphere. It also may be that models with the source near the photosphere lead to spicules appearing to be suspended (e.g., the spicules may appear at the heights of shock formation), but this has yet to be verified. It may be that the spicules only appear to be suspended due to, e.g., obscuration at low heights by low lying features (Bray et al. 1974, Gaizauskas 1984), although Gaizauskas (1984) argues against this.
- Are the suspected twisting motions in spicules real, and if so, how common are they, and are the twists oscillatory? This has direct implications for the low-frequency Alfvén wave models, or the unwinding flux-rope scenarios.
- Can high-frequency Alfvén wave fluctuations be detected, which may indicate that the ion-neutral friction mechanism suggested by Haerendel (1992) may be acting?
- Are there any signatures at the root of spicules indicating their initiation source? As mentioned earlier, Suematsu et al. (1995) found that chromospheric bright points appear after spicule-like structures are already extended, rather than prior to their onset. It would be desirable to repeat these observations with higher resolution, and for a wider category of features.
- Does a large percentage of spicules “fade from view” when observed in $H\alpha$ (e.g., Lippincott 1957; Beckers 1968, Beckers 1972), or are most of them similar to the spicule-like structures seen by Suematsu et al. (1995), which rise and fall?
- What occurs at the footpoints of spicules? What are the velocities of the magnetic flux-tube elements (filigree) in the photosphere? Are these features the footpoints of spicules? Or maybe the footpoints correspond to canceling magnetic features?
- Do spicules originate from unipolar regions, as suggested by the observations of Suematsu et al. (1995)? Or will improved resolution reveal that their bases consist of more complex magnetic elements, perhaps supporting a reconnection picture, or the core-field eruption scenario of Moore et al. (1999)?
- What is the relation between $H\alpha$ spicules and UV and EUV spicules, macrospicules, surges, and X-ray jets, etc.? Will observations support a similar or identical generating mechanism for some or all of these phenomena?

These are just a sample of the many questions that should be addressed in order to help to refine, or revolutionize, spicule models.

High resolution ($1''$) in the UV and EUV range is currently available with the *TRACE* mission. Those data can be used to refine properties of, for example, C IV spicules, and eventually their relation with chromospheric spicules. Also, it will be informative to investigate further the *TRACE* 171 Å “dark inclusions” features, and the “moss” features mentioned earlier. These should be compared with C IV spicule observations, and with $H\alpha$ spicule observations if possible.

We are hopeful that the upcoming Solar-B mission—a Japanese project with US and UK participation—will provide reliable answers to many of the outstanding observational

questions regarding spicules and related features. Currently, plans call for Solar-B to be launched in 2004, and to carry a 50 cm-diameter-primary solar optical telescope (SOT), an EUV imaging spectrometer (EIS), and a grazing-incidence soft X-ray telescope (XRT).

If SOT achieves the hoped-for spatial resolution of $\lesssim 0.25''$, it will no doubt vastly improve our spicule knowledge. Equipped with a narrow band (≈ 100 mÅ) tunable Lyot filter, it will be able to scan the H α line from, say, H α $- 1.0$ Å to H α $+ 1.0$ Å, taking images at a rapid cadence (on the order of seconds). This will allow for virtually simultaneous movies at a number of wavelength positions of spicules. It will be important to carry out these observations optimized for both limb spicules, and disk features. Studies of these data will tell us much about the physical properties and dynamics of these features. Analyzing the full set of these line-scan movies will reveal Doppler information on the evolution of these features. Although spicules radiate simultaneously in different chromospheric lines, such as various H, He, and Ca lines (e.g., see the reviews listed in §2, and also Pasachoff et al. 1968), some differences do appear at the different wavelengths. SOT will be able to tell us more about these similarities and differences by observing spicules in various (yet to be determined) chromospheric lines in addition to H α .

By appropriately pre-setting exposure durations while observing the limb, it should be possible to make similar data sets scanning the H α line, where a subset of the images are optimized for disk features and another subset is optimized for limb spicules. It should be possible rapidly alternate these settings in order to image features straddling the limb—ones that both partially reside on disk and partially protrude beyond the limb—helping to identify the disk counterpart(s) to spicules. SOT will also be capable of generating high-resolution ($\lesssim 0.25''$) magnetograms. These will be useful to compare with the source regions of spicule-like disk structures.

Prospects for EIS observations of UV or EUV spicules are more modest, due to the instrumental spatial resolution, which is $2''$, with $1''$ pixels. Some spicule-like features should still be visible at this resolution, however, as discussed by Dere et al. (1983) and as exemplified by *SOHO* EIT He 304 Å images. EIT has resolution similar to that expected for EIS and does show some jet-like features at the limb. Comparisons with the SOT images therefore should address some of the questions of the relation between the chromospheric spicules and transition region spicule-like features. EIS will observe the 256 Å He II lower-transition region line, which has a formation temperature of about 10^5 K, similar to that of C IV. EIS' spectral resolution should allow for detection of line-broadening-associated velocities of order 10 km s $^{-1}$, allowing observations of “explosive events” seen by the NRL HRTS experiment (e.g., Dere et al. 1983, Dere et al. 1991) and the SUMER instrument on *SOHO* (e.g., Chae et al. 1998). XRT will have spatial resolution similar to that of EIS. Comparing SOT observations with EIS and XRT observations should show if the relations between cool features (e.g., “gas plugs”) and hot features (X-ray jets, X-ray and UV microflare brightenings) predicted by the Sterling et al. 1991, 1993, 1994) simulations hold, in addition to telling us more about the relationships between surges and X-ray features (e.g., Schmieder et al. 1988; Shibata et al. 1992). EIS also is expected to see hotter transition region and coronal lines, which will also make interesting comparisons with the SOT images.

High resolution, atmospheric effects-free observations are vital for a full description of the spicule phenomenon. Such observations will have to support the appropriate set of model predictions before any of the models examined here—or any future model—can be deemed “correct.”

This work was supported by the National Research Council, while the author held an NRC—NASA/MSFC Research Associateship. The work was also supported in part by the NRL/ONR basic research program, while the author was employed by Computational Physics Inc., Fairfax, VA, and located at the Institute of Space and Astronautical Science, Sagami-hara, Japan. The author thanks J. V. Hollweg, H. S. Hudson, P. Martins, R. L. Moore, K. Shibata, and Y. Suematsu for useful insight and discussions.

References

- Ajmanova, G. K., Ajmanova, A. K., and Gulyaev, R. A. 1982, *Solar Phys.*, 79, 323.
- Andreev, A. S. 1996, *Astro. Lett. and Communications*, 34, 145.
- Athay, R. G. 1984, *ApJ*, 287, 412.
- Athay, R. G. 1976, *The Solar Chromosphere and Corona: Quiet Sun* (Dordrecht:Reidel).
- Athay, R. G., and Holzer, T. E. 1982, *ApJ*, 255, 743.
- Athay, R. G., and Thomas, R. N. 1957, *ApJ*, 125, 804.
- Beckers, J. M. 1968, *Solar Phys.*, 3, 367.
- Beckers, J. M. 1972, *Ann. Rev. Astron. Astro.*, 10, 73.
- Belcher, J. W., and Davis, L. Jr. 1971, *JGR*, 76, 3534.
- Belien, A. J. C., Martens, P. C. H., Keppens, R. 1999, *ApJ*, 526, 478.
- Berger, T. E., de Pontieu, B., Schrijver, C. J., and Title, A. M. 1999, *ApJ*, 519, 97.
- Bhavilal, R. 1965, *MNRAS*, 130, 411.
- Blake, M. L., and Sturrock, P. A. 1985, *ApJ*, 290, 359.
- Bohlin, J. D., Vogel, S. N., Purcell, S. N., Sheeley, N. R., Tousey, R., and Van Hoosier, M. E. 1975, *ApJ*, 197, L133.
- Bonnet, R. M., Decaudin, M., Bruner, E. C., Jr., Acton, L. W., and Brown, W. A. 1980, *ApJ*, 237, 47.
- Braun, D., and Lindsey, C. 1987, *ApJ*, 320, 898.
- Bray, R. J. 1969, *Solar Phys.*, 10, 63.
- Bray, R. J., and Loughhead, R. E. 1974, *The Solar Chromosphere* (London:Chapman and Hall).
- Brueckner, G. E., Bartoe, J.-D. F. 1983, *ApJ*, 272, 329.
- Brueckner, G. E., Bartoe, J.-D. F., Cook, J. W., Dere, K. P., Socker, D. G., Kurokawa, H., and McCabe, M. 1986, *Adv. Space Res.*, 6, 263.
- Budnik, F., Schroeder, K.-P., Wilhelm, K., and Glassmeier, K.-H. 1998, *Astron. Astrophys.*, 334, L77.
- Campos, L. M. B. C. 1984, *MNRAS*, 207, 547.
- Canfield, R. C., Reardon, K. P., Leka, K. D., Shibata, K., Yokoyama, T., and Shimojo, M. 1996, *ApJ*, 464, 1016.
- Cargill, P. J., Spicer, D. S., and Zalesak, S. T. 1997, *ApJ*, 488, 854.
- Carlsson, M., and Stein, R. F. 1995, *ApJ*, 440, L29.
- Carlsson, M., and Stein, R. F. 1997, *ApJ*, 481, 500.
- Carlsson, M., Judge, P. G., and Wilhelm, K. 1997, *ApJ*, 486, L63.
- Chae, J., Wang, H., Lee, Chik-Yin, and Goode, P. R. 1998, *ApJ*, 504, L123.
- Cheng, Q.-Q. 1992c, *Astron. Astrophys.*, 262, 581.
- Cheng, Q.-Q. 1992a, *Astron. Astrophys.*, 266, 537.
- Cheng, Q.-Q. 1992b, *Astron. Astrophys.*, 266, 549.

- Cook, J. W., Brueckner, G. E., Bartoe, J.-D. F., and Socker, D. G. 1984, *Adv. Space Res.* 4, 59.
- Cook, J. W. 1991, in *Mechanisms of Chromospheric and Coronal Heating*, (Springer-Verlag), ed. Ulmschneider, P., Priest, E. R., and Rosner, R., p. 83.
- Cram, L. E. 1985, in *Chromospheric Diagnostics and Modeling*, NSO Conf. (ed. B. W. Lites) Sacramento Peak, Sunspot, p. 53.
- Cuny, Y. 1987, *Astron. Astrophys.*, 175, 243.
- de Pontieu, B. 1996, PhD Thesis, University of Ghent, Belgium
- de Pontieu, B., and Haerendel, G. 1998, *Astron. Astrophys.*, 338, 729.
- de Pontieu, B. 1999, *Astron. Astrophys.*, 347, 696.
- Dere, K. P., Bartoe, J.-D. F., and Brueckner, G. E. 1983, *ApJ*, 267, L65.
- Dere, K. P., Bartoe, J.-D. F., Brueckner, G. E., Cook, J. W., Socker, D. G., and Ewing, J. W. 1989, *Solar Phys.*, 119, 55.
- Dere, K. P., Bartoe, J.-D. F., and Brueckner, G. E., Ewing, J., and Lun, P. 1991, *J. Geophys. Res.*, 96, 9399.
- Feldman, U. 1983, *ApJ*, 275, 367.
- Fontenla, J. M., Tandberg-Hanssen, E., Reichmann, E. J., and Filipowski, S. 1989, *ApJ*, 344, 1034.
- Foukal, P. V. 1971, *Solar Phys.*, 19, 59.
- Foukal, P. V. 1990, *Solar Astrophysics* (Wiley:New York).
- Gaizauskas, V. 1984, *Solar Phys.*, 93, 257.
- Gaizauskas, V. 1985, in *Chromospheric Diagnostics and Modeling*, NSO Conf. (ed. B. W. Lites) Sacramento Peak, Sunspot, p. 25.
- Gaizauskas, V. 1996, *Solar Phys.*, 169, 367.
- Gallagher, P. T., Phillips, K. J. H., Harra-Murnion, L. K., Baudin, F., and Keenan, F. P. 1999, *Astron. Astrophys.*, 348, 251.
- Georgakilas, A. A., Koutchmy, S., and Alissandrakis, C. E. 1999, *Astron. Astrophys.*, 341, 610.
- Gibson, E. G. 1973, *The Quiet Sun*, NASA SP-303 (Washington, D.C.).
- Giovanelli, R. G. 1978, *Solar Phys.*, 59, 293.
- Grossmann-Doerth, U. and Schmidt, W. 1992, *Astron. Astrophys.*, 264, 236.
- Habbal, S. R., and Gonzalez, R. D. 1991, *ApJ*, 376, L25.
- Haerendel, G. 1992, *Nature*, 360, 241.
- Hansteen, V. H., and Wikstol, O. 1994, *Astron. Astrophys.*, 290, 995.
- Hasan, S. S., and Keil, S. L. 1984, *ApJ*, 283, L75.
- Heinzel, P. and Schmieder, B. 1994, *Astron. Astrophys.*, 282, 939.
- Hasan, S. S., and Venkatakrishnan, P. 1981, *Solar Phys.*, 73, 45.
- Henoux, J. C., and Somov, B. V. 1997, *Astron. Astrophys.*, 318, 947.
- Heristchi, D., and Mouradian, Z. 1992, *Solar Phys.*, 142, 21.
- Hirayama, T. 1992, *Solar Phys.*, 37, 33.
- Hollweg, J. V. 1972, *Cosmic Electrodynamics*, 2, 423.
- Hollweg, J. V., and Lee, M. A. 1989, *GRL*, 16, 919.
- Hollweg, J. V. 1982, *ApJ*, 257, 345.
- Hollweg, J. V. 1992, *ApJ*, 389, 731.
- Hollweg, J. V., Jackson, S., and Galloway, D. 1982, *Solar Phys.*, 75, 35.
- Judge, P., Carlsson, M., and Wilhelm, K. 1997, *ApJ*, 490, L195.

- Karovska, M., Blundell, S. F., and Habbal, S. R. 1994, *ApJ*, 428, 854.
- Karovska, M. and Habbal, S. R. 1994, *ApJ*, 431, L59.
- Karpen, J. T., Antiochos, S. K., and DeVore, C. R. 1995, *ApJ*, 450, 422.
- Kudoh, T. and Shibata, K. 1999, *ApJ*, 514, 493.
- Kopp, R. A., and Kuperus, M. 1968, *Solar Phys.*, 4, 212.
- Kuperus, M., and Athay, R. G. 1967, *Solar Phys.*, 1, 361.
- Kundu, M. R., Raulin, J. P., Nitta, N., Hudson, H. S., Shimojo, M., Shibata, K., and Raoult, A. 1995, *ApJ*, 447, 135.
- Kundu, M. R., Raulin, J.-P., Nitta, N., Shibata, K., and Shimojo, M. 1998, *Solar Phys.*, 178, 611.
- Kundu, M. R., Nindos, A., Raulin, J.-P., Shibasaki, K., White, S. M., Nitta, N., Shibata, K., Shimojo, M. 1999, *ApJ*, 520, 391.
- LaBonte, B. J. 1979, *Solar Phys.*, 61, 283.
- Landman, D. A. 1984, *ApJ*, 284, 833.
- Lippincott, S. L. 1957, *Smithson. Contrib. Ap.*, 2, 15.
- Livshits, M. A. 1967, *Soviet Astron.—AJ*, 10, 570.
- Lorrain, P. and Koutchmy, S. 1996, *Solar Phys.*, 165, 115.
- Loucif, M. L. 1994, *Astron. Astrophys.*, 281, 95.
- Loughhead, R. E. 1969, *Solar Phys.*, 10, 71.
- Lynch, D. K., Beckers, J. M., and Dunn, R. B. 1973, *Solar Phys.* 30, 63.
- Mariska, J. T. 1992, *The Solar Transition Region* (New York:Cambridge University Press).
- Mariska, J. T., and Hollweg, J. V. 1985, 296, 746.
- Matsuno, K., and Hirayama, T. 1988, *Solar Phys.*, 117, 21.
- Michard, R. 1974, in *Chromospheric Fine Structure* (G. Athay, ed.) (IAU), p. 3.
- Moore, R. L. and Fung, P. C., W. 1972, *Solar Phys.*, 23, 78.
- Moore, R. L., Tang, F., Bohlin, J. D., and Golub, L. 1977, *ApJ*, 218, 286.
- Moore, R. L., Falconer, D. A., Porter, J. G., and Suess, S. T. 1999, *ApJ*, 526, 505.
- Morse, P. M., and Feshbach, H. 1953, *Methods of Theoretical Physics* (New York:McGraw-Hill), Section 11.1.
- Nagai, F. 1980, *Solar Phys.*, 68, 351.
- Nagai, F., and Emslie, A. G. 1984, *ApJ*, 279, 896.
- Narain, U. and Ulmschneider, P. 1990, *Space Sci. Rev.*, 54, 377.
- Narain, U. and Ulmschneider, P. 1996, *Space Sci. Rev.*, 75, 453.
- Nishikawa, T. 1988, *PASJ*, 40, 613.
- Nikolsky, G. M. 1970, *Solar Phys.*, 12, 379.
- Nikol'skii, G. M., and Sazanov, A. A. 1967, *Soviet Astron.-A.J.*, 10, 744.
- Osterbrock, D. E. 1961, *ApJ*, 134, 347.
- Papushev, P. G. 1980, *Solar Phys.*, 68, 275.
- Pasachoff, J. M., Noyes, R. W., and Beckers, J. M. 1968, *Solar Phys.*, 5, 131.
- Pataraya, A. D., Taktakishvili, A. L., and Chargeishvili, B. B. 1990, *Solar Phys.*, 128, 333.
- Piddington, J. H. 1956, *Mon. Not. R. astr. Soc.*, 116, 314.
- Pike, C. D., and Mason, H. E. 1998, 182, 333.
- Pneuman, G. W., and Kopp, R. A. 1978, *Solar Phys.*, 57, 49.
- Poletto, G. 1980, *ApJ*, 240, L69.
- Poletto, G. 1981, *Solar Phys.*, 73, 233.
- Porter, J. G., Moore, R. L., Reichmann, E. J., Engvold, O., and Harvey, K. L. 1987, *ApJ*,

323, 380.

- Rabin, D., and Moore, R. L. 1980, *ApJ*, 241, 394.
- Rae, I. C., and Roberts, B. 1982, *ApJ*, 256, 761.
- Roberts, B. 1979, *Solar Phys.*, 61, 23.
- Roberts, B., and Mangeney, A. 1982, *MNRAS*, 198, 7.
- Roudier, Th., Espagnet, O., Muller, R., and Vigneau, J. 1994, *Astron. Astrophys.*, 287, 982.
- Roy, J.-R. 1973, *Solar Phys.*, 32, 139.
- Rush, J. H., and Roberts, W. O. 1954, *Aust. J. Phys.*, 7, 230.
- Rust, D. M., et al. 1980, in *Solar Flares, Skylab Workshop II*, ed. P. Sturrock (Boulder: Colorado Assoc. Univ. Press), 273.
- Schatten, K. H., and Mayr, H. G. 1986, *ApJ*, 309, 864.
- Schmieder, B., Simnett, G. M., Tandberg-Hanssen, E., and Mein, P. 1988, *Astron. Astrophys.*, 201, 327.
- Schmieder, B., Shibata, K., Van Driel-Gesztelyi, L., and Freeland, S. 1995, *Solar Phys.*, 156, 245.
- Schmieder, B., Golub, L., and Antiochos, S. K. 1996, *ApJ*, 425, 326.
- Shibata, K. 1982, *Solar Phys.*, 81, 9.
- Shibata, K. 1983, *PASJ*, 35, 263.
- Shibata, K., and Suematsu, Y. 1982, *Solar Phys.*, 78, 333.
- Shibata, K., Nishikawa, T., Kitai, R., and Suematsu, Y. 1982, *Solar Phys.*, 77, 121.
- Shibata, K., and Uchida, Y. 1986, *Solar Phys.*, 103, 299.
- Shibata, K., et al. 1992, *PASJ*, 44, L173.
- Shibata, K., et al. 1994, *ApJ*, 431, L51.
- Shimojo, M., Hashimoto, S., Shibata, K., Hirayama, T., Hudson, H. S., and Acton, L. W. 1996, *PASJ*, 48, 123.
- Solanki, S. K., Livingston, W., Muglach, K., and Wallace, L. 1996, *Astron. Astrophys.*, 315, 303.
- Solanki, S. K. 1998, in *Solar Jets and Coronal Plumes*, ed. T.-D. Guyenne, (SP-421) (Noordwijk: ESA), 115.
- Steiner, O., Grossmann-Doerth, U., Knoelker, M., and Schussler, M. 1998, *ApJ*, 495, 468.
- Steinolfson, R. S., Schmahl, E. J., and Wu, S. T. 1979, *Solar Phys.*, 63, 187.
- Sterling, A. C. 1998a, in *Solar Jets and Coronal Plumes*, ed. T.-D. Guyenne, (SP-421) (Noordwijk: ESA), 35.
- Sterling, A. C. 1998b, *ApJ*, 508, 916.
- Sterling, A. C., and Hollweg, J. V. 1984, *ApJ*, 285, 843.
- Sterling, A. C., and Hollweg, J. V. 1988, *ApJ*, 327, 950.
- Sterling, A. C., and Hollweg, J. V. 1989, *ApJ*, 343, 985.
- Sterling, A. C., and Mariska, J. T. 1990, *ApJ*, 349, 647.
- Sterling, A. C., Mariska, J. T., Shibata, K., and Suematsu, Y. 1991, *ApJ*, 381, 313.
- Sterling, A. C., Shibata, K., and Mariska, J. T. 1993, *ApJ*, 407, 778.
- Sterling, A. C., Shibata, K., and Mariska, J. T. 1994, *Space Science Reviews*, 70, 77.
- Strong, K. T., Harvey, K., Hirayama, T., Nitta, N., Shimizu, T., Tsuneta, S. 1992, *PASJ*, 44, L161.
- Suematsu, Y., Shibata, K., Nishikawa, T., and Kitai, R. 1982, *Solar Phys.*, 75, 99.
- Suematsu, Y. 1985, *Solar Phys.*, 98, 67.
- Suematsu, Y. 1990, in *Lecture Notes in Physics 367, Progress of Seismology of the Sun and*

- Stars, ed. Y. Osaki and H. Shibahashi (Berlin:Springer), 211.
- Suematsu, Y. and Takeuchi, A. 1991, in *Lecture Notes in Physics* 387, Flare Physics in Solar Activity. Maximum 22, ed. Y. Uchida, R. C. Canfield, T. Watanabe, and E. Hiei, 259
- Suematsu, Y., Wang, H., Zirin, H. 1995, *ApJ*, 450, 411.
- Suematsu, Y. 1998, in *Solar Jets and Coronal Plumes*, ed. T.-D. Guyenne, (SP-421) (Noordwijk: ESA), 19.
- Tanaka, K. 1974, in *Chromospheric Fine Structure* (G. Athay, ed.) (IAU), p. 239.
- Tarbell, T., Ryutova, M., Covington, J., and Fludra, A. 1999, *ApJ*, 514, 47L.
- Thomas, R. N. and Athay, R. G. 1961, *Physics of the Solar Chromosphere*, Interscience, New York.
- Tsiropoula, G., Alissandrakis, C. E., Schmieder, B. 1994, *Astron. Astrophys.*, 290, 285.
- Tsiropoula, G., and Schmieder, B. 1997, *Astron. Astrophys.*, 324, 1183.
- Tsirul'nik, L. B. 1984, *Sov. Astron.*, 27(4), 411.
- Unno, W., Ribes, E., and Appenzeller, I. 1974, *Solar Phys.*, 35, 287.
- Velli, M., and Liewer, P. 1999, *Space Sci. Rev.*, 87, 339.
- Wang, H. 1998, *ApJ*, 509, 461.
- Wang, J., et al. 2000, *ApJ*, in press.
- Weart, S. R. 1970, *Solar Phys.*, 14, 310.
- Withbroe, G. L. 1983, *ApJ*, 267, 825.
- Withbroe, G. L. et al. 1976, *ApJ*, 203, 528.
- Yokoyama, T., and Shibata, K. 1995, *Nature*, 375, 42.
- Yokoyama, T., and Shibata, K. 1996, *PASJ*, 48, 353.
- Zachariadis, Th. G., Georgakilas, A. A., Koutchmy, S., and Alissandrakis, C. E. 1999, *Solar Phys.*, 184, 77.
- Zirin, H. 1988, *Astrophysics of the Sun*, Cambridge University Press
- Zirker, J. B. 1967, *Solar Phys.*, 1, 204.